Journal of Cleaner Production 509 (2025) 145530

Contents lists available at ScienceDirect

Journal of Cleaner Production

journal homepage: www.elsevier.com/locate/jclepro

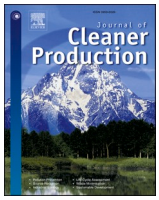

Harnessing cow manure waste for nanocellulose extraction and sustainable small-structure manufacturing

Yanqi Dai [a,1], Dongyang Sun [b,1], Dominic O'Rourke [b], Sasireka Velusamy [c], Senthilarasu Sundaram [c,*], Mohan Edirisinghe [a,**]

[a] Department of Mechanical Engineering, University College London, London, WC1E 7JE, UK
[b] Department of Engineering, School of Computing, Engineering and the Built Environment, Edinburgh Napier University, Merchiston Campus, Edinburgh, EH10 5DT, UK
[c] Department of Engineering, School of Computing, Engineering and Digital Technologies, Teesside University, Tees Valley, Middlesbrough, TS1 3BX, UK

ARTICLE INFO

Handling Editor: Zhen Leng

Keywords:
Natural resource
Biopolymer
Nanofibril
Spinning
Waste recycling

ABSTRACT

The use of sustainable materials as alternatives to fossil-derived materials is vital to tackle the current environmental challenges. Cellulose is a good candidate due to its intrinsic properties. It is wise to consider cellulose rich-waste materials as its sources, rather than high-grade resources, integrating with the concept of a circular economy. In this study, we successfully produced type I cellulose nanofibrils with an average diameter of 12.8 ± 4.1 nm, from cow manure collected from a local dairy farm, leveraging this sustainable cellulose source to upscale agricultural waste into high-performance biopolymers. This new route offers a practical solution to provide an abundant source of cellulose feedstock while mitigating the environmental concerns of farm animal waste. Following this, the extracted cellulose was used for manufacturing small-structure cellulose products through an innovative method, namely nozzle-pressurized spinning. This is distinguished by its simplicity, high efficiency, and low-energy consumption for straightforward forming. The morphological diversity of these cellulose products further expands their application fields, such as textile, food additives, packaging, electronics, and healthcare.

1. Introduction

As global concerns regarding the depletion of non-renewable resources and environmental challenges continue to escalate, exploring environmentally friendly material sources and corresponding processing techniques has become a growing emphasis within both scientific research and industrial production. Utilizing natural materials not only mitigates environmental issues associated with material synthesis and disposal but also ensures a stable resource supply, thereby aligning with market demands and circular economy concepts. Proper waste handling is the essential factor for the next generation of renewable resources for many industries, especially the farming sector. This can be effectively recycled into useful materials for diverse areas spanning energy storage (Yu and Manthiram, 2021), composite manufacturing (Lunetto et al., 2023), biomedicine and healthcare (Chin et al., 2023), optoelectronics, and beyond.

Cellulose, a naturally occurring material, can be a good candidate for the above purpose due to its inherent biodegradability, suitable mechanical and thermal properties, inherent hydrophilicity, controllable porosity, and non-toxicity (Trache et al., 2020). Nanocellulose, mainly referring to cellulose nanofibrils in this article, typically exhibits nanoscale dimensions with diameters ranging from 5 to 60 nm and lengths up to several micrometers, giving it a high aspect ratio and surface area (Klemm et al., 2011). These properties contribute to its remarkable tensile strength, which can exceed 2 GPa, and its stiffness, with Young's modulus comparable to steel (about 140 GPa) (Jakob et al., 2022; Šturcová et al., 2005). Such characteristics make nanocellulose an excellent reinforcement material in composites, improving their mechanical strength, flexibility, and durability. Furthermore, its ability to form hydrogen bonds and interact with other materials enhances the performance of eco-friendly films and coatings. These attributes, combined with its biodegradability and renewability, position nanocellulose as a versatile material for diverse applications (Carolin C et al., 2023; Ghamari et al., 2024).

* Corresponding author.
** Corresponding author.
E-mail addresses: S.Sundaram@tees.ac.uk (S. Sundaram), m.edirisinghe@ucl.ac.uk (M. Edirisinghe).
[1] Contributed equally.

https://doi.org/10.1016/j.jclepro.2025.145530
Received 16 August 2024; Received in revised form 5 April 2025; Accepted 13 April 2025
Available online 15 April 2025

While cellulose has conventionally been sourced from botanical constituents such as wood, plant stems, and leaves, recent efforts have turned towards exploring alternative sources through waste recycling streams that are rich in cellulose content (Antony and thottiam Vasudevan, 2018; Chandrasekar et al., 2024; Honda et al., 2002; Liu et al., 2020; Ogundare et al., 2017; Yousef et al., 2019). This approach not only prolongs the use cycles of materials but also effectively mitigates the environmental impact of waste disposal, integrating with the concept of circular economy. Agricultural residues, e.g. rice straw and bagasse fibers, have received much attention due to their functionalities that are very similar to hardwood cellulose (Padhi et al., 2023). While extensive research has been conducted on nanocellulose derived from plant-based sources, there is limited exploration of animal waste, such as horse manure, cow manure, and elephant manure (Weiland et al., 2021, 2023; Yang et al., 2023), highlighting their feasibility in nanocellulose production. These organic wastes contain partially digested plant fibers, making them a promising yet unconventional raw material for sustainable nanocellulose extraction. However, this area of research is still in its early stages, with challenges such as low extraction efficiency and the presence of residual impurities posing significant obstacles to progress.

Dairy farm waste such as cow manure/dung is a major threat to the environment especially in polluting water bodies and contributing to waterborne diseases and public health hazards (Berendes et al., 2018). Manure waste releases significant amounts of greenhouse gases (GHGs) such as methane (CH_4), carbon dioxide (CO_2), and nitrous oxide (N_2O), contributing to climate change (Petersen et al., 2013). Additionally, the decomposition of organic matter in manure emits ammonia (NH_3), which can lead to acid rain and particulate matter formation, adversely affecting air quality and human health (Nieder and Benbi, 2022). Animal manure harbor a diverse range of bacterial, viral, and protozoan pathogens, including *Escherichia coli*, *Salmonella* spp., *Shigella* spp., *Campylobacter jejuni*, *Vibrio cholerae*, rotaviruses, noroviruses, *Giardia* spp., *Cryptosporidium* spp., and *Entamoeba histolytica* (Leclerc et al., 2002). These pathogens pose significant risks to human health, primarily through the transmission of serious infectious diseases. Intestinal infections are among the most common outcomes, leading to acute diarrhea, chronic health issues, and even life-threatening conditions in vulnerable populations (Berendes et al., 2017, 2018). These health impacts can often occur through direct or indirect contact with fecal matter, emphasizing the critical need for effective waste management to mitigate risks. In regions where agriculture and animal husbandry prevail, animal waste such as cow manure, finds utility as crop fertilizer, fuel, or house insulation material (Gupta et al., 2016). With further research into animal waste, there is growing interest in recovering valuable substances, such as nanocellulose, from these waste materials for refinement into high-value products, thereby finding applications across diverse fields (Ghamari et al., 2024). In food packaging, its transparency, strength, and excellent barrier properties against oxygen and moisture enable the development of sustainable, biodegradable alternatives to plastic (Bideau et al., 2017). In energy storage, the high surface area and network-forming capability of nanocellulose make it ideal as a binder, separator, or component in lightweight and flexible devices such as batteries and supercapacitors (Kim et al., 2016). Similarly, its flexibility, dielectric properties, and compatibility with functional materials position it as a key material for electronics, including substrates and dielectric layers in field-effect transistors (FETs) (Cunha et al., 2017; Huang et al., 2013). In biomedicine, nanocellulose stands out for its biocompatibility, high water retention, and capacity for functionalization, supporting applications in wound dressings, drug delivery systems, and tissue engineering scaffolds (Ao et al., 2017; Miao et al., 2011; Yusefi et al., 2022). There are very few reports on the conversion of cow manure as a feedstock for nanocellulose considering these undigested materials consist of cellulose (1.6–23.5 %), hemicellulose (1.4–12.8 %), and lignin (2.7–13.9 %) (Chen et al., 2003). Our recent research has identified that cow manure has been a good fit into the circular economy due to its abundance, low cost, and great potential to address waste management challenges associated with animal husbandry. The extracted nanocellulose, however, has not been utilized, but in this work, we use it to manufacture small-structure films, ribbons, and fibers for specific applications using an innovative spinning method–Nozzle-pressurized spinning (NPS). Conventional NPS incorporates vertical axis rotation. In this work, we used a modified frame of NPS where rotation was around a horizontal axis and incorporated a water bath.

In conjunction with sustainable raw material sources, the advance of low-energy and high-efficiency processing techniques stands as an essential requisite in promoting the realization of "Waste to Wealth" idea in a circular economy. NPS, also known as nozzle-pressurized gyration, was proposed as a promising strategy, revolutionizing the manufacture of small-structure materials with remarkable efficiency through a straightforward process (Dai et al., 2022). NPS is mechanically driven by a centrifugal force and assisted by a high-pressure nitrogen flow for ejecting polymer jets that subsequently form fine fibers as the solvent evaporates. Compared with the prevailing spinning technologies, NPS eliminates the high energy consumption, constraints on sensitive materials, and safety-related concerns associated with the high-voltage electric field in electrospinning (Amarakoon et al., 2023; Dai et al., 2023; Heseltine et al., 2018). Additionally, NPS significantly enhances spinning efficiency by generating multiple jets at once. When compared to centrifugal spinning, the introduction of gas flow in NPS not only further refines the morphology but also makes it better suited for handling highly viscous spinning feedstock like those of sodium alginate, cellulose, chitin, and other biopolymers. Compared with other fiber-forming technologies such as phase separation, template synthesis, and self-assembly, NPS offers the benefits of simple equipment and easy operation, enabling continuous spinning of long fibers.

In this work, the upcycling of farm waste was achieved by extracting nanocellulose from cow manure through chemical reactions and mechanical homogenization. The extracted cellulose subsequently served as the spinning feedstock for modified NPS. These pressure-spun cellulose products hold the potential of becoming high value-added commodities due to the inherent characteristics of the material and the surface effects of their small structure, thereby realizing the concept of "Waste to Wealth". In addition to natural and sustainable raw materials, the entire processing procedure avoided the use/production of chemicals or waste that pose significant environmental hazards and was simple, efficient, and low-cost, in line with the requirements of a circular economy.

2. Materials and methods

2.1. Raw materials and chemicals

The raw cow manure sample was firstly dried in the open air, followed by oven drying at 105 °C overnight for disinfection. The dried cow manure crust was then ground and sieved to a smaller particle size. Glacial acetic acid (CH_3COOH), sodium hypochlorite solution (NaClO, 6–14 % active chlorine), sodium chloride (NaCl), sodium hydroxide (NaOH), 1-ethyl-3-methylimidazolium acetate (EMIM OAc) and dimethyl sulfoxide (DMSO) were obtained from Sigma-Aldrich UK. A mixture of EMIM OAc and DMSO with a mass ratio of 1:1 was used as the solvent for cellulose in this work. All chemicals were reagent grade and used without further purification. Ultrapure water (Pure lab Option-Q, Class 1 water system, ELGA) was used in all the experiments.

2.1.1. Field emission scanning electron microscopy (FE-SEM)

The morphology of cellulose nanofibrils extracted from the cow manure sample was examined using S4800 FE-SEM (Hitachi, Japan). The sample solution was collected on a freshly cleaved mica disc (muscovite, 9.9 mm diameter and 0.22–0.27 mm thickness, Agar Scientific, UK) that was attached on an FE-SEM aluminum stub. The sample was dried overnight at room temperature (≈20 °C) before gold coated

for 90 s using a sputter coater (EMITECH K550X, Quorumtech, UK) and observed with the FE-SEM at 3 kV acceleration voltage. ImageJ software was used for the fibril width measurement using micrographs of 45k magnifications.

The size and morphology of the resulting cellulose products from modified NPS were examined using GeminiSEM 360 (ZEISS, Germany). The preparation of imaging samples followed the above procedures and observations were conducted at an acceleration voltage of 1 kV. From the acquired SEM images, the diameters of the cellulose fibers were quantified using ImageJ and subsequently plotted and analyzed with OriginPro.

2.1.2. X-ray diffraction (XRD)

The X-ray diffraction patterns were recorded with D8 Advance X-ray diffractometer (Bruker, Germany) by using Cu-K radiation ($\lambda = 0.1542$ nm), a parallel beam with Gobel mirror, and a Dynamic Scintillation detector. The accelerating voltage was 40 kV with a current of 30 mA, and the scanning range was between 5° and 40° (2 theta).

2.1.3. Fourier-transform infrared spectroscopy (FTIR)

The extracted nanocellulose samples were dried into films and used to obtain the spectrum between the 4000–450 cm^{-1} range at 4 cm^{-1} resolution. The functional groups of the nanocellulose samples processed for 0, 5, 10, 15, and 20 passes (0 p, 5 p, 10 p, and 20 p) were determined using the FTIR spectrophotometer (Spectrum 100, PerkinElmer, UK) and are shown in Supplementary Table 1.

2.2. Nanocellulose extraction

The extraction procedure was adopted from previous studies where a different biomass was used as the feedstock (Sun et al., 2020). Briefly, the nanocellulose extraction started with a bleaching process, where the dried cow manure particles were placed in an acidified NaClO solution (3 wt%) at room temperature and stirred overnight for delignification of the material. The sample was then processed in a NaOH aqueous solution (1 wt%) in ambient conditions with constant stirring for 2 h. An extra delignification process was used subsequently by placing the sample in the same NaClO solution as above for 2 h under continuous stirring. The material was washed vigorously in ultrapure water between each step by successive centrifugation and decantation. A detailed description of the procedure is provided in Supplementary 2. Methodology.

The above material was mixed with pure water obtaining a slurry with a solid content of approximately 0.25 wt% and homogenized using a rotor-stator mixer (Ultra-turrax T 25, IKA, UK) for approximately 10 min at 13000 rpm. The slurry was then subjected to a homogenization process using a PSI-20 homogenizer (Adaptive Instruments, UK) through a 200 μm Z-shaped interaction chamber at approximately 8000 psi. This process was repeated a different number of times and the samples were identified as being processed for 0, 5, 10, 15, and 20 passes. Fig. 1 presents the experimental workflow for cellulose extraction and fiber spinning.

2.3. Conductometric titration

Conductometric titration was carried out to measure the total residual carboxy group content on two representative cellulose samples before and after the homogenization process (0 p and 20 p samples). During the tests, 100 mg of oven-dried sample was dispersed to 55 mL d H_20 and 5 mL 0.01 M NaCl. The solution was adjusted to have a pH between 2.5 and 3.0 using 0.1 M HCl and left mixing for 1 h. Samples were titrated with 0.04 M NaOH at a rate of 100 μL/min until pH 11 was reached. Conductivity and pH were recorded with each titration addition. The data was plotted shown in Supplementary Fig. 1, and V_1 and V_2 intersect were calculated using R software. Carboxyl content was calculated using Equation (1):

$$C = \frac{(V_2 - V_1) \times C_{NaOH}}{m} \quad (1)$$

Where C is the total carboxyl content of the sample, V_1 and V_2 are the volume of NaOH consumed at the first and second intersect, in liters, respectively; C_{NaOH} is the concentration of NaOH used, in moles, and m is oven-dry weight of the sample, in grams.

2.4. Water retention values (WRV) and sedimentation experiments

The water retention values were examined in order to indirectly evaluate the degree of fibrillation for the samples that were processed for 0, 5, 10, 15, and 20 passes in the homogenization process. 50 g of the slurry was transferred into falcon tubes and subjected to a centrifugation process, using a reported method (Cheng et al., 2010). The material was centrifuged at 900 G for 30 min; thereafter, the supernatant was decanted, and the remaining slurry was weighed before and after drying in an oven overnight. The WRV was evaluated using Equation (2):

$$WRV = \frac{W_{wet} - W_{dry}}{W_{dry}} \times 100 \quad (2)$$

Where W_{wet} and W_{dry} are the weight of the wet slurry and the dried material, respectively. Three replicates were examined and an average WRV was obtained.

A sedimentation test was completed to study the degree of fibrillation during the homogenization process. 0 p, 5 p, 10 p, 15 p, and 20 p samples of 0.25 wt% slurries were allowed to sediment for at least 72 h, in a glass vial of 60 mL, before being photographed. The material in the picture was measured using ImageJ to get the initial height (h_0) and sentiment height (h_s) to obtain the relative sediment height (h_s/h_0).

2.5. Production of cellulose fibers using modified nozzle-pressurized spinning

The solid content of the nanocellulose extraction was subsequently used as the feedstock for modified NPS. The dry nanocellulose was obtained through freeze-drying the slurry from the preceding steps, which was then dissolved in EMIM OAc/DMSO at different solid ratios to form a series of homogeneous cellulose solutions with concentration gradients (2, 4, 6, 8, and 10 wt%). DMSO as a cosolvent promotes the dissolution of cellulose in EMIM OAc, providing an efficient and

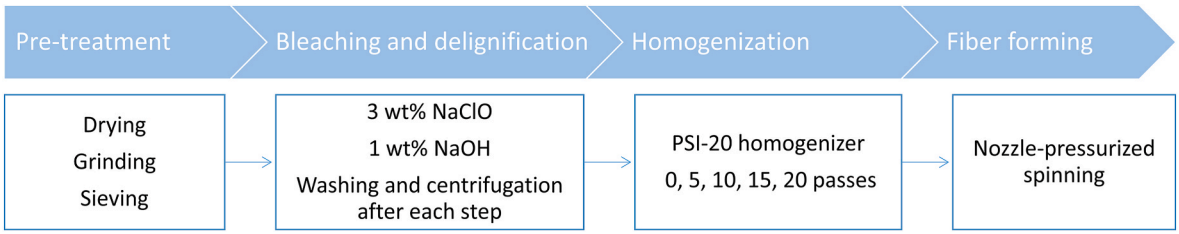

Fig. 1. Flowchart depicting the cellulose extraction and forming process.

environmentally friendly approach to cellulose dissolution. The dissolution process was further promoted by gentle heating (≈40 °C) and prolonged mechanical stirring (≈48 h). The viscosity of the prepared cellulose solutions was measured at ambient temperature by a Brookfield Viscosity-meter. These solutions were then subjected to a modified NPS setup.

The diagram illustrating the optimized NPS setup can be found in Fig. 2. An aluminum vessel, a cylindrical container with a diameter of 60 mm and a height of 30 mm, was designed as the chamber for introducing the spinning feedstock. The vessel is equipped with eight external nozzles, each with an inner diameter of 0.3 mm and a length of 5 mm, to facilitate precise feedstock delivery. It is connected to an electric motor capable of reaching rotational speeds of up to 12000 rpm. Additionally, a nitrogen cylinder is linked to the vessel via a plastic tube, supplying a working pressure inside the vessel chamber of up to 0.3 MPa. Rotational speed and working pressure are two major system parameters in NPS, significantly influencing the formation, morphology, and yield of fiber production. Rotational speed imparts a centrifugal force to the loaded feedstock, enabling it to overcome surface tension and extrude from the nozzles. The working pressure further assists this process, particularly beneficial for materials of exceptionally high viscosity.

Finding the optimal system parameters is crucial for jet formation (Fig. 3a). Insufficient rotational speed and working pressure may result in feedstock retention in the chamber, whereas excessive rotational speed and working pressure can lead to a jet split into droplets (Fig. 3b). However, spinning cellulose fibers using typical NPS presents a challenge because of the struggle to detach solvents from cellulose, owing to the strong hydrogen bonds. To address this issue, a water bath is incorporated into the NPS setup. Wet spinning of cellulose can be achieved by this combination.

Following preliminary testing, the cellulose solutions prepared above were subjected to the modified NPS setup. The working conditions were as follows: rotational speed of 12000 rpm, working pressure of 0.3 MPa, and the distance from the nozzle tip to the water bath surface (air gap length) was 10 mm. The spinning was performed at ambient temperature (≈20 °C) and relative humidity of 40–45 %. The cellulose solutions were spun into the water bath and allowed to coagulate in water for 5 h. The water was replaced every hour to remove the solvent as much as possible. Afterward, the cellulose samples were removed from the water and placed in an oven at 55 °C until completely dried.

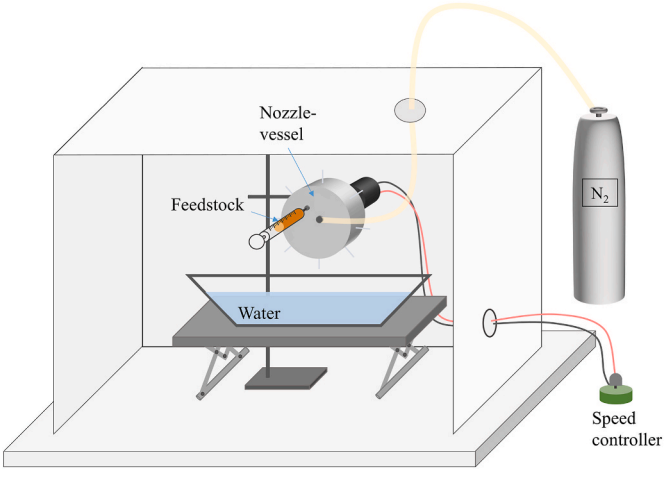

Fig. 2. Schematic of modified nozzle-pressurized spinning incorporating a water bath. Rotation takes place around a horizontal axis.

3. Results and discussions

3.1. Extraction of cellulose from cow dung

An effective conversion from cow dung waste to cellulose slurries can be seen in Fig. 4. After the dried cow manure crust was ground and sieved (Fig. 4a), it was treated in NaClO and NaOH solutions respectively. During this process, lignin, hemicellulose, and other organic substances, such as proteins, fats, carbohydrates, and other bioorganic molecules, that are not part of the cellulose structure, were removed, resulting in a white-colored cellulose slurry (Fig. 4b). All reactions were completed under ambient conditions to eliminate possible cellulose hydrolysis due to excessive processing in the NaOH solution. Fig. 4c–f shows the slurries of cellulose that were obtained using the homogenization process of 5, 10, 15, and 20 passes, respectively. The consistency of the slurries is dramatically increased, which shows the evolution of the homogenization of cellulose.

3.2. Structural and conductometric titration analysis

The Fourier transform infrared spectroscopy (FTIR) spectrum of the cow manure-derived cellulose was measured at different numbers of passes (Fig. 5a). All spectra show the typical bands corresponding to the functional groups present in the cellulose molecular structure, including O–H stretching (3334–3340 cm^{-1}), C–H stretching (2901–2927 cm^{-1}), and C–O stretching (1032–1035 cm^{-1}) (Dai et al., 2024; Onyianta et al., 2018). Notably, these functional groups remain unchanged with an increasing number of passes, indicating that the chemical integrity of the cellulose is preserved throughout the process. The detailed identification of peaks and their assignment in the cellulose structure are summarized in Supplementary Table 1. The presence of a characteristic peak around 1640 cm^{-1} confirms the obtained cellulose remains in the original, unmodified form. If surface modifications, such as esterification or amidation—typically occurring during chemical pre-treatment in the cellulose derivation process—had taken place, a peak shift to approximately 1740 cm^{-1} or 1590 cm^{-1}, respectively, would be observed (Onyianta et al., 2018). Thus, no significant surface modifications were detected in the obtained cellulose in this study.

Two cellulose samples before and after the homogenization process (0 p and 20 p) were further studied by conductimetric titration analysis. The total carboxyl group content for the two samples is 260 and 284 μg/mol, respectively. This shows that the level of carboxymethylation is relatively consistent during the transition from the coarse fiber fragments to nano-fibrillated cellulose during the high-shear homogenization. The total carboxyl group content for the cow manure cellulose samples in this work is higher than the wood-based samples processed in our previous work (Sun et al., 2020), although it is still lower than surface-modified cellulose. The slightly higher value of the sample may be attributed to the change during the two NaClO bleaching processes, known to partially oxidize the cellulose hydroxyl groups to aldehyde/-carboxylic acid groups (Someshwar and Pinkerton, 1992). It is also speculated that because the fiber source in the original animal feed has been ingested and digested, which acts as a "mechanical, acidic and enzyme pre-treatment'' of sorts, the standard extraction processes of this feedstock will become more potent than normal, thus giving the higher carboxyl content.

Fig. 5b shows the X-ray diffractograms for the nanocellulose sample after 20 passes. The diffraction peaks identified at 2θ of 16.5°, 22.2°, and 34.5° correspond to the (110), (200), and (004) crystallographic planes of cellulose I (Reddy et al., 2018). Some work in the literature has reported that when a high concentration of NaOH is used in the extraction process, the derived cellulose can change from type I to II (Moreno et al., 2020). This is not the case in our work which depicts that the 1 % NaOH solution is suitable for the cellulose extraction process without converting its crystalline structure.

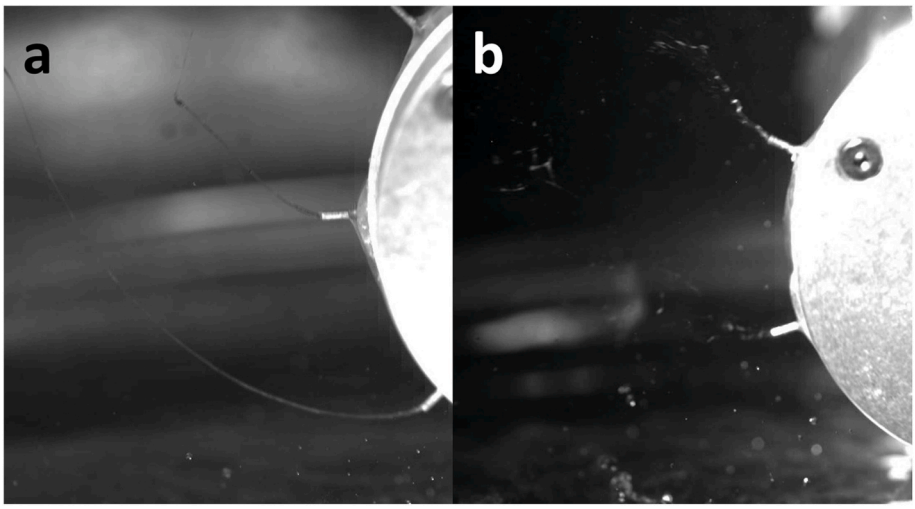

Fig. 3. Digital photos of (a) spinning jets and (b) jet rupture captured by a high-speed camera.

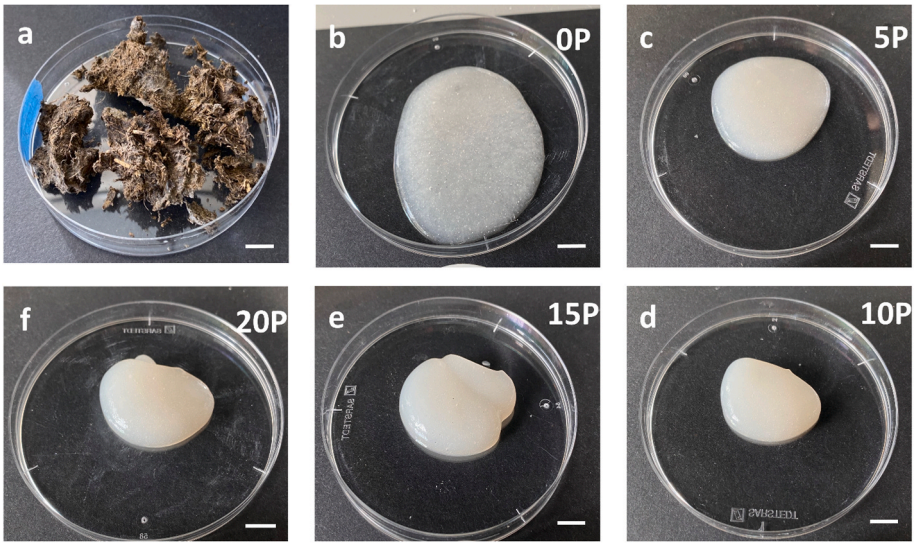

Fig. 4. Photographs of (a) dried cow dung crust, (b) cellulose slurry after extraction, and (c–f) the cellulose material obtained using the homogenization process of 5, 10, 15, and 20 passes, respectively. (Scale = 10 mm).

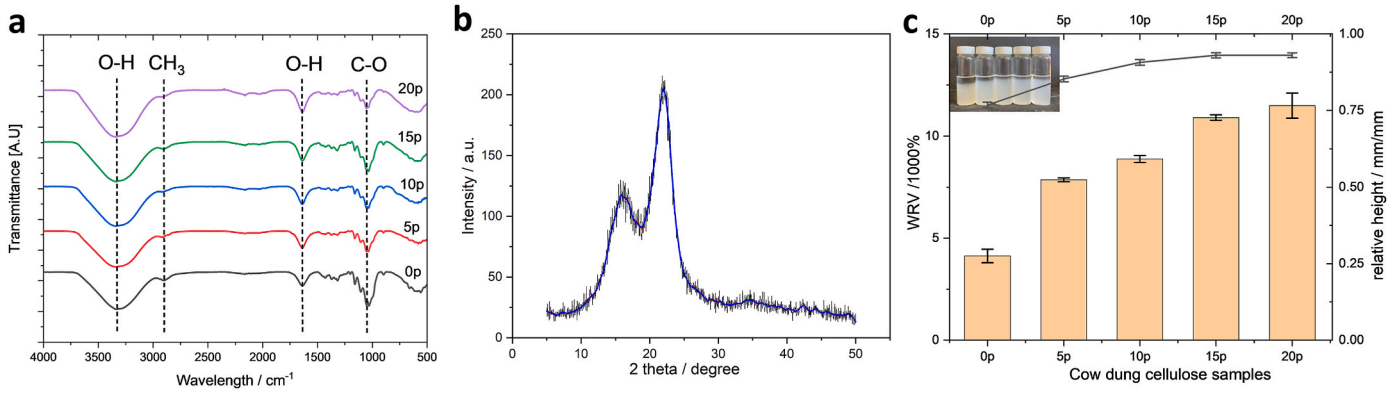

Fig. 5. (a) FTIR spectra of cow manure cellulose that were homogenized at 0, 5, 10, 15, and 20 passes, assigned with characteristic peaks. (b) XRD pattern for nanocellulose extracted using cow manure after 20 passes of homogenization. (c) Effects of increased number of passes on water retention values and sedimentation properties.

3.3. Water retention values and sedimentation properties

The WRV result for samples of the various number of passes is shown in Fig. 5c. A clear tendency can be seen that as the number of passes increases during the homogenization process, the water retention capacity of the sample is also increased. Cellulose has high hygroscopicity due to the interaction of its hydroxyl groups with water molecules (Cheng et al., 2010). When cellulose materials are subjected to the homogenizer, more individualized fibrils are formed through the fiber delamination process, thus the total surface area is increased. As a result, more hydroxyl groups become accessible to interact with water molecules which can be bonded to the cellulose surface. The greatest increase can be seen between 0 p and 5 p samples, indicating that a substantial fibril delamination happened at this step, although such an increasing trend becomes exponential thereafter showing the delamination was still progressing but at a slower extent and gradually moving towards saturation. This is possibly because as the process goes on, the larger-sized fibers are delaminated to form smaller fibrils until a stage when most of the small fibrils are hardly delaminated further under the existing shear force. Therefore, it can be predicted that even if the samples were to be processed further (e.g. beyond 20 passes), the increase in WRV would be insignificant.

A similar saturation trend can be observed in the graph of relative sediment height (h_s/h_0) vs. the number of passes for cellulose samples in Fig. 5c. As indicated in the inset photograph, cellulose fibrils in the slurry sediment due to its own gravity. However, as the aspect ratio of the fibrils increases (more nanofibrils are delaminated from larger fibers), a more complex 3D fibril network can be formed to prohibit their sedimentation. Therefore, a good linear proportional relationship can be established between the number of passes and the relative sediment height, which can be used to indirectly evaluate the degree of fibrillation of cellulose during the homogenization process. The plateau of the graph amongst samples of a greater number of passes shows a similar phenomenon as explained in the WRV work.

3.4. Morphological analysis of cellulose nanofibrils

Micrographs (Fig. 6) show the microstructure of cellulose nanofibrils after processing for 20 passes. No large fragments of fibers can be seen in the sample which can be commonly present in other nanocellulose materials processed using plant materials reported in previous work (Sun et al., 2020). During the process, the material passed through an interaction chamber at approximately 400 m/s, where a substantial shear force was applied to the cellulose fibers, resulting in their delamination to form nanoscale fibrils. The long nature of individual fibrils is also evident, which can be greater than 1 μm. Such a high length could result in the formation of a web-like network structure (Fig. 6a and b) which is similar to the morphology of cellulose samples reported elsewhere (Chinga-Carrasco, 2011). The width of individual fibrils from the above sample was measured and the distribution was summarized in Fig. 6c. The histogram evidenced that the width distribution is asymmetrical and in the range between 5 and 35 nm approximately. The mean fibril width is 12.8 ± 4.1 nm.

3.5. Processing cellulose using modified nozzle-pressurized spinning

Fig. 7 exhibits the morphology of cellulose before and after processing with modified NPS. The freeze-dried nanocellulose is observed to aggregate into flakes (Fig. 7a), which are much larger in size than the cellulose fibrils, losing the characteristic nano-structure of nanofibrils (Fig. 6). Fig. 7b–e illustrate the gradual transformation of the sample morphology after NPS processing as the cellulose concentration increases from 2 wt% to 10 wt%, respectively. Initially, the cellulose formed a thin film at the lowest concentration, which then split into broad ribbons, and finally refined further to form thin filaments with the increase in cellulose concentration. In Fig. 7b, the surface roughness of the cellulose film may be attributed to the viscosity scatter in the solution resulting from impurities present in the extracted cellulose. The inset shows the cross-section of the film with a thickness of approximately 5 μm. Fig. 7f suggests that the diameter distribution of the cellulose fibers obtained from the 10 wt% solution follows a Gaussian distribution, with an average diameter of 5.2 ± 2.3 μm. Similarly, this relatively large variance in fiber diameter may be caused by viscosity scatter resulting from impurities.

As the processing parameters associated with modified NPS remained consistent, the variations observed in cellulose morphology can be attributed to the difference in solution viscosity caused by the concentration difference (Gericke et al., 2009; Quan et al., 2010; Tan et al., 2016). The relationship between these two variables is depicted in Fig. 8. For concentrations below 4 wt%, the cellulose solutions have very low viscosity, indicating their high fluidity. Consequently, despite being extruded from the NPS in the form of a jet (Fig. 3a), the cellulose solutions rapidly flowed and dispersed into a uniform film after entering the water bath. Coagulation has not yet occurred at this stage. With further increases in concentration, the cellulose solution experiences a notable rise in viscosity, signifying a decrease in its fluidity. Because of this, the flow and interdiffusion of the cellulose jets in the water bath became restricted. Coagulation occurred before they fully spread out, thereby resulting in the formation of broad ribbon-like cellulose samples. The solution fluidity further deteriorated after the concentration reached 8 wt% due to the exceptionally high viscosity. Therefore, coagulation occurred while the jets maintained the filament-like morphology the jet

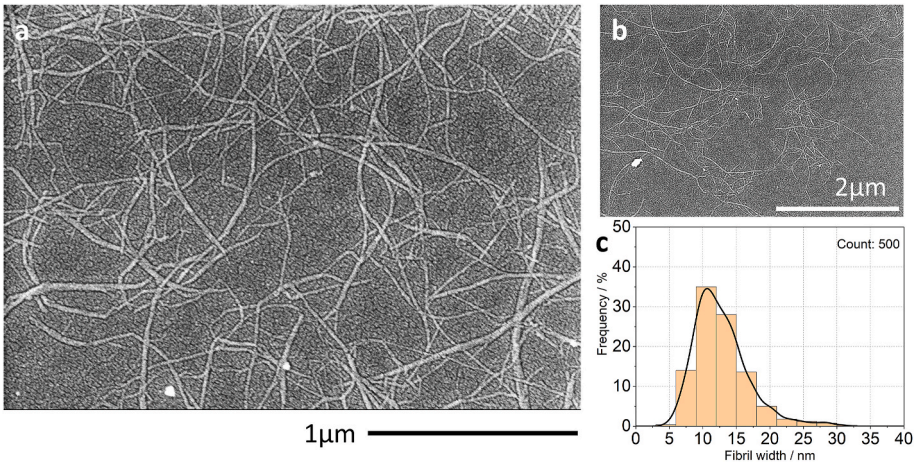

Fig. 6. FE-SEM images of nanofibrils from cow mature at (a) 45k and (b) 25k magnifications. (c) The fibril width distribution of cellulose nanofibrils.

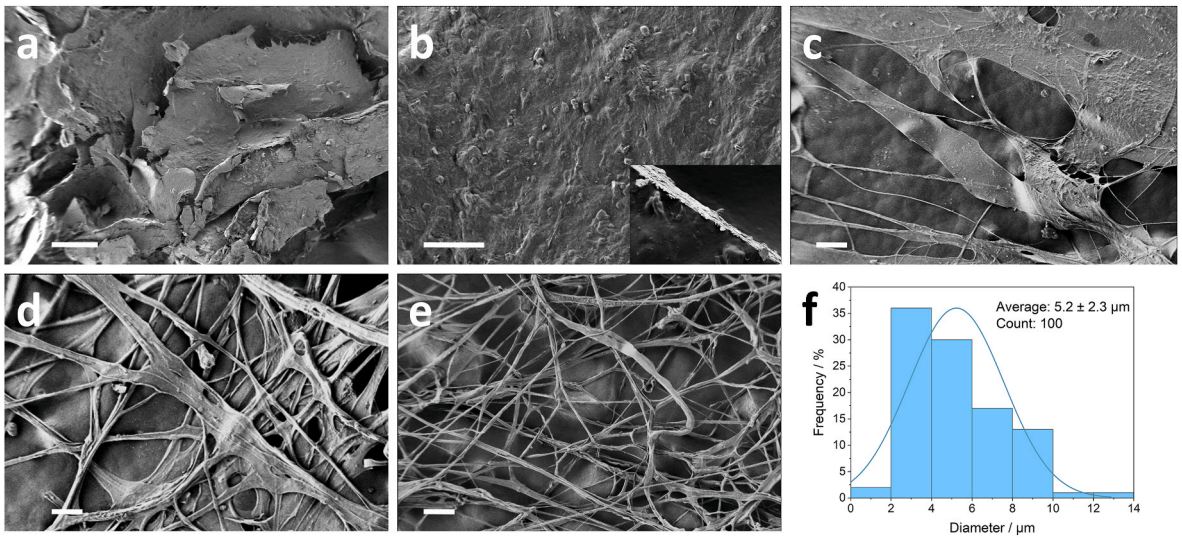

Fig. 7. SEM images of (a) dried nanocellulose and (b–e) cellulose samples produced by modified NPS from solutions with concentrations of (b) 2 wt%, (c) 4 wt%, (d) 8 wt%, (e) 10 wt%. (f) The diameter distribution of cellulose fibers produced from the 10 wt% solution. (Scale bar = 100 μm).

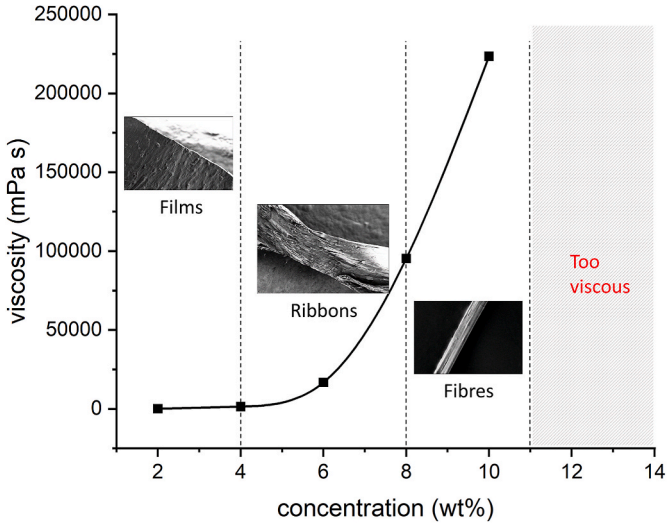

Fig. 8. The viscosity profile of cellulose solutions and the structures of corresponding products.. (solutions with a concentration of higher than 11 wt% are excessively viscous to be processed.)

adopted upon extruding from the nozzle tip (Fig. 3a), resulting in the formation of cellulose fibers. Therefore, choosing the appropriate solution concentration is crucial for achieving the desired morphology of cellulose products. This information can be obtained from Fig. 8.

4. Conclusions

The upcycling of cow manure into nanocellulose is achieved through a mild chemical reaction and homogenization, yielding cellulose nanofibrils approximately 12.8 nm in diameter. Functional group analysis confirms the cellulose structure remains unchanged with increased processing passes, while XRD analysis identifies it as type I cellulose. Water retention and sedimentation height plateau after multiple passes of homogenization, highlights effective processing. The findings highlight the feasibility of repurposing dairy farm waste as a sustainable cellulose source, aligning with circular economy principles. The use of EMIM OAc solvent further enhances the environmental benefits by enabling solvent recyclability and reducing reliance on hazardous chemicals. The versatility of the extracted cellulose, capable of forming films, ribbons, and fibers down to micro-scale via the modified NPS method, underscores its potential in diverse applications, such as packaging, energy storage, electronics, and biomedicine.

Despite its promising potential, research in this area remains in its early stages. The scalability of the process requires further evaluation, particularly regarding cost-effectiveness, cellulose yield, and large-scale solvent recovery. Future research will focus on optimizing process efficiency and gaining deeper insights into the functional performance of the extracted cellulose to broaden its applicability. By addressing these challenges, this approach could significantly contribute to sustainable material production and waste valorization in the bioeconomy.

CRediT authorship contribution statement

Yanqi Dai: Writing – review & editing, Writing – original draft, Methodology, Formal analysis, Conceptualization. **Dongyang Sun:** Writing – original draft, Methodology, Conceptualization. **Dominic O'Rourke:** Methodology, Formal analysis. **Sasireka Velusamy:** Methodology, Formal analysis. **Senthilarasu Sundaram:** Supervision, Conceptualization. **Mohan Edirisinghe:** Supervision, Conceptualization.

Declaration of competing interest

The authors declare that they have no known competing financial interests or personal relationships that could have appeared to influence the work reported in this paper.

Acknowledgments

YD is supported by China Scholarship Council (CSC) for her PhD studies at University College London. We thank UKRI for funding the core pressurized spinning research at UCL (Grants: EP/S016872/1, EP/N034228/1, EP/L023059/1). The authors would also like to thank School of Engineering and Built Environment, Edinburgh Napier University who supported some of the experimental work.

Appendix A. Supplementary data

Supplementary data to this article can be found online at https://doi.org/10.1016/j.jclepro.2025.145530.

Data availability

Data will be made available on request.

References

Amarakoon, M., Homer-Vanniasinkam, S., Edirisinghe, M., 2023. A global challenge: sustainability of submicrometer PEO and PVP fiber production. Global Challenges 7 (9), 2300152. https://doi.org/10.1002/gch2.202300152.

Antony, A., thottiam Vasudevan, R., 2018. A review on cellulose and its utilization from agro-industrial waste. Drug Invent. Today 10, 89–94.

Ao, C., Niu, Y., Zhang, X., He, X., Zhang, W., Lu, C., 2017. Fabrication and characterization of electrospun cellulose/nano-hydroxyapatite nanofibers for bone tissue engineering. Int. J. Biol. Macromol. 97, 568–573.

Berendes, D., Leon, J., Kirby, A., Clennon, J., Raj, S., Yakubu, H., Robb, K., Kartikeyan, A., Hemavathy, P., Gunasekaran, A., Roy, S., Ghale, B.C., Kumar, J.S., Mohan, V.R., Kang, G., Moe, C., 2017. Household sanitation is associated with lower risk of bacterial and protozoal enteric infections, but not viral infections and diarrhoea, in a cohort study in a low-income urban neighbourhood in vellore, India. Trop. Med. Int. Health 22 (9), 1119–1129. https://doi.org/10.1111/tmi.12915.

Berendes, D.M., Yang, P.J., Lai, A., Hu, D., Brown, J., 2018. Estimation of global recoverable human and animal faecal biomass. Nat. Sustain. 1 (11), 679–685. https://doi.org/10.1038/s41893-018-0167-0.

Bideau, B., Bras, J., Adoui, N., Loranger, E., Daneault, C., 2017. Polypyrrole/Nanocellulose composite for food preservation: barrier and antioxidant characterization. Food Packag. Shelf Life 12, 1–8. https://doi.org/10.1016/j.fpsl.2017.01.007.

Carolin C, F., Kamalesh, T., Kumar, P.S., Hemavathy, R.V., Rangasamy, G., 2023. A critical review on sustainable cellulose materials and its multifaceted applications. Ind. Crop. Prod. 203, 117221. https://doi.org/10.1016/j.indcrop.2023.117221.

Chandrasekar, C.M., Carullo, D., Saitta, F., Krishnamachari, H., Bellesia, T., Nespoli, L., Caneva, E., Baschieri, C., Signorelli, M., Barbiroli, A.G., Fessas, D., Farris, S., Romano, D., 2024. Valorization of citrus peel industrial wastes for facile extraction of extractives, pectin, and cellulose nanocrystals through ultrasonication: an in-depth investigation. Carbohydr. Polym. 344, 122539. https://doi.org/10.1016/j.carbpol.2024.122539.

Chen, S., Liao, W., Liu, C., Wen, Z., Kincaid, R.L., Harrison, J.H., Elliott, D.C., Brown, M. D., Solana, A.E., Stevens, D.J., 2003. Value-Added Chemicals from Animal Manure. https://citeseerx.ist.psu.edu/document?repid=rep1&type=pdf&doi=0824e70e75aeb19e9c08ed74771b0b813f8332ef.

Cheng, Q., Wang, J., McNeel, J., Jacobson, P., 2010. Water retention value measurements of cellulosic materials using a centrifuge technique. Bioresources 5. https://doi.org/10.15376/biores.5.3.1945-1954.

Chin, M.H.W., Linke, J., Coppens, M.-O., 2023. Nature-inspired sustainable medical materials. Curr. Opinion Biomed. Eng. 28, 100499. https://doi.org/10.1016/j.cobme.2023.100499.

Chinga-Carrasco, G., 2011. Cellulose fibres, nanofibrils and microfibrils: the morphological sequence of MFC components from a plant physiology and fibre technology point of view. Nanoscale Res. Lett. 6. https://doi.org/10.1186/1556-276x-6-417. Article 417.

Cunha, I., Barras, R., Grey, P., Gaspar, D., Fortunato, E., Martins, R., Pereira, L., 2017. Reusable cellulose-based hydrogel sticker film applied as gate dielectric in paper electrolyte-gated transistors. Adv. Funct. Mater. 27 (16), 1606755. https://doi.org/10.1002/adfm.201606755.

Dai, Y., Ahmed, J., Delbusso, A., Edirisinghe, M., 2022. Nozzle-pressurized gyration: a novel fiber manufacturing process. Macromol. Mater. Eng. 307 (9), 2200268. https://doi.org/10.1002/mame.202200268.

Dai, Y., Ahmed, J., Edirisinghe, M., 2023. Pressurized gyration: fundamentals, advancements, and future. Macromol. Mater. Eng. 308 (7), 2300033. https://doi.org/10.1002/mame.202300033.

Dai, Y., Sun, D., Sundaram, S., Delbusso, A., O'Rourke, D., Dorris, M., Edirisinghe, M., 2024. Facile synthesis: from laminaria hyperborea to cellulose films and fibers. Cellulose 31 (1), 205–216. https://doi.org/10.1007/s10570-023-05606-w.

Gericke, M., Schlufter, K., Liebert, T., Heinze, T., Budtova, T., 2009. Rheological properties of cellulose/ionic liquid solutions: from dilute to concentrated states. Biomacromolecules 10 (5), 1188–1194. https://doi.org/10.1021/bm801430x.

Ghamari, M., Sun, D., Dai, Y., See, C.H., Yu, H., Edirisinghe, M., Sundaram, S., 2024. Valorization of diverse waste-derived nanocellulose for multifaceted applications: a review. Int. J. Biol. Macromol. 280, 136130. https://doi.org/10.1016/j.ijbiomac.2024.136130.

Gupta, K.K., Aneja, K.R., Rana, D., 2016. Current status of cow dung as a bioresource for sustainable development. Biores. Bioprocess. 3 (1), 28. https://doi.org/10.1186/s40643-016-0105-9.

Heseltine, P.L., Ahmed, J., Edirisinghe, M., 2018. Developments in pressurized gyration for the mass production of polymeric fibers. Macromol. Mater. Eng. 303 (9), 1800218. https://doi.org/10.1002/mame.201800218.

Honda, S.i., Miyata, N., Iwahori, K., 2002. Recovery of biomass cellulose from waste sewage sludge. J. Mater. Cycles Waste Manag. 4 (1), 46–50. https://doi.org/10.1007/s10163-001-0054-y.

Huang, J., Zhu, H., Chen, Y., Preston, C., Rohrbach, K., Cumings, J., Hu, L., 2013. Highly transparent and flexible nanopaper transistors. ACS Nano 7 (3), 2106–2113. https://doi.org/10.1021/nn304407r.

Jakob, M., Mahendran, A.R., Gindl-Altmutter, W., Bliem, P., Konnerth, J., Müller, U., Veigel, S., 2022. The strength and stiffness of oriented wood and cellulose-fibre materials: a review. Prog. Mater. Sci. 125, 100916. https://doi.org/10.1016/j.pmatsci.2021.100916.

Kim, J.-H., Gu, M., Lee, D.H., Kim, J.-H., Oh, Y.-S., Min, S.H., Kim, B.-S., Lee, S.-Y., 2016. Functionalized nanocellulose-integrated heterolayered nanomats toward smart battery separators. Nano Lett. 16 (9), 5533–5541. https://doi.org/10.1021/acs.nanolett.6b02069.

Klemm, D., Kramer, F., Moritz, S., Lindström, T., Ankerfors, M., Gray, D., Dorris, A., 2011. Nanocelluloses: a new family of nature-based materials. Angew. Chem. Int. Ed. 50 (24), 5438–5466. https://doi.org/10.1002/anie.201001273.

Leclerc, H., Schwartzbrod, L., Dei-Cas, E., 2002. Microbial agents associated with waterborne diseases. Crit. Rev. Microbiol. 28 (4), 371–409.

Liu, B., Li, T., Wang, W., Sagis, L.M.C., Yuan, Q., Lei, X., Cohen Stuart, M.A., Li, D., Bao, C., Bai, J., Yu, Z., Ren, F., Li, Y., 2020. Corncob cellulose nanosphere as an eco-friendly detergent. Nat. Sustain. 3 (6), 448–458. https://doi.org/10.1038/s41893-020-0501-1.

Lunetto, V., Galati, M., Settineri, L., Iuliano, L., 2023. Sustainability in the manufacturing of composite materials: a literature review and directions for future research. J. Manuf. Process. 85, 858–874. https://doi.org/10.1016/j.jmapro.2022.12.020.

Miao, J., Pangule, R.C., Paskaleva, E.E., Hwang, E.E., Kane, R.S., Linhardt, R.J., Dordick, J.S., 2011. Lysostaphin-functionalized cellulose fibers with antistaphylococcal activity for wound healing applications. Biomaterials 32 (36), 9557–9567.

Moreno, L.M., Gorinstein, S., Medina, O.J., Palacios, J., Muñoz, E.J., 2020. Valorization of garlic crops residues as precursors of cellulosic materials. Waste Biomass Valor. 11 (9), 4767–4779. https://doi.org/10.1007/s12649-019-00799-3.

Nieder, R., Benbi, D.K., 2022. Reactive nitrogen compounds and their influence on human health: an overview. Rev. Environ. Health 37 (2), 229–246.

Ogundare, S.A., Moodley, V., van Zyl, W.E., 2017. Nanocrystalline cellulose isolated from discarded cigarette filters. Carbohydr. Polym. 175, 273–281. https://doi.org/10.1016/j.carbpol.2017.08.008.

Onyianta, A., Dorris, M., Williams, R., 2018. Aqueous morpholine pre-treatment in cellulose nanofibril (CNF) production: comparison with carboxymethylation and TEMPO oxidisation pre-treatment methods. Cellulose 25, 1–18. https://doi.org/10.1007/s10570-017-1631-0.

Padhi, S., Singh, A., Routray, W., 2023. Nanocellulose from agro-waste: a comprehensive review of extraction methods and applications. Rev. Environ. Sci. Biotechnol. 22 (1), 1–27. https://doi.org/10.1007/s11157-023-09643-6.

Petersen, S.O., Blanchard, M., Chadwick, D., Del Prado, A., Edouard, N., Mosquera, J., Sommer, S.G., 2013. Manure management for greenhouse gas mitigation. Animal 7 (s2), 266–282.

Quan, S.-L., Kang, S.-G., Chin, I.-J., 2010. Characterization of cellulose fibers electrospun using ionic liquid. Cellulose 17 (2), 223–230. https://doi.org/10.1007/s10570-009-9386-x.

Reddy, K.O., Maheswari, C.U., Dhlamini, M.S., Mothudi, B.M., Kommula, V.P., Zhang, J., Zhang, J., Rajulu, A.V., 2018. Extraction and characterization of cellulose single fibers from native African napier grass. Carbohydr. Polym. 188, 85–91. https://doi.org/10.1016/j.carbpol.2018.01.110.

Someshwar, A.V., Pinkerton, J., 1992. Wood processing industry. In: Air Pollution Engineering Manual, vol. 844. https://p2infohouse.org/ref/33/32354.pdf.

Šturcová, A., Davies, G.R., Eichhorn, S.J., 2005. Elastic modulus and stress-transfer properties of tunicate cellulose whiskers. Biomacromolecules 6 (2), 1055–1061. https://doi.org/10.1021/bm049291k.

Sun, D., Onyianta, A.J., O'Rourke, D., Perrin, G., Popescu, C.-M., Saw, L.H., Cai, Z., Dorris, M., 2020. A process for deriving high quality cellulose nanofibrils from water hyacinth invasive species. Cellulose 27 (7), 3727–3740. https://doi.org/10.1007/s10570-020-03038-4.

Tan, X., Li, X., Chen, L., Xie, F., 2016. Solubility of starch and microcrystalline cellulose in 1-ethyl-3-methylimidazolium acetate ionic liquid and solution rheological properties [10.1039/C6CP04426C]. Phys. Chem. Chem. Phys. 18 (39), 27584–27593. https://doi.org/10.1039/C6CP04426C.

Trache, D., Tarchoun, A.F., Derradji, M., Hamidon, T.S., Masruchin, N., Brosse, N., Hussin, M.H., 2020. Nanocellulose: from fundamentals to advanced applications. Front. Chem. 8, 392. https://doi.org/10.3389/fchem.2020.00392.

Weiland, K., Alge, K., Mautner, A., Bauer, A., Bismarck, A., 2023. Horse manure as resource for biogas and nanolignocellulosic fibres. Bioresour. Technol. 372, 128688. https://doi.org/10.1016/j.biortech.2023.128688.

Weiland, K., Wlcek, B., Krexner, T., Kral, I., Kontturi, E., Mautner, A., Bauer, A., Bismarck, A., 2021. Excellence in excrements: upcycling of herbivore manure into nanocellulose and biogas. ACS Sustain. Chem. Eng. 9 (46), 15506–15513. https://doi.org/10.1021/acssuschemeng.1c05175.

Yang, X., Li, L., Zhao, W., Wang, M., Yang, W., Tian, Y., Zheng, R., Deng, S., Mu, Y., Zhu, X., 2023. Characteristics and functional application of cellulose fibers extracted from cow dung wastes. Materials 16 (2), 648. https://www.mdpi.com/1996-1944/16/2/648.

Yousef, S., Hamdy, M., Tatariants, M., Tuckute, S., El-Abden, S.Z., Kliucininkas, L., Baltusnikas, A., 2019. Sustainable industrial technology for recovery of cellulose from banknote production waste and reprocessing into cellulose nanocrystals. Resour. Conserv. Recycl. 149, 510–520. https://doi.org/10.1016/j.resconrec.2019.06.026.

Yu, X., Manthiram, A., 2021. Sustainable battery materials for next-generation electrical energy storage. Adv. Energy Sustain. Res. 2 (5), 2000102. https://doi.org/10.1002/aesr.202000102.

Yusefi, M., Soon, M.L.-K., Teow, S.-Y., Monchouguy, E.I., Neerooa, B.N.H.M., Izadiyan, Z., Jahangirian, H., Rafiee-Moghaddam, R., Webster, T.J., Shameli, K., 2022. Fabrication of cellulose nanocrystals as potential anticancer drug delivery systems for colorectal cancer treatment. Int. J. Biol. Macromol. 199, 372–385.